Volume 1 | Number 1 | Jan 2013 | Pages 1–100

Dalton Transactions

An international journal of inorganic chemistry
www.rsc.org/dalton

ROYAL SOCIETY OF CHEMISTRY

ROYAL SOCIETY OF CHEMISTRY

www.rsc.org/dalton

Journal Name

RSCPublishing

COMMUNICATION

Graphic Abstract

Thermal conversion of a tailored metal-organic framework into lithium silicate with an unusual morphology for efficient CO_2 capture

Jae Hwa Lee,[a] Byoungnam Moon,[a] Tae Kyung Kim,[a] Sungeun Jeoung,[a] and Hoi Ri Moon*[a]
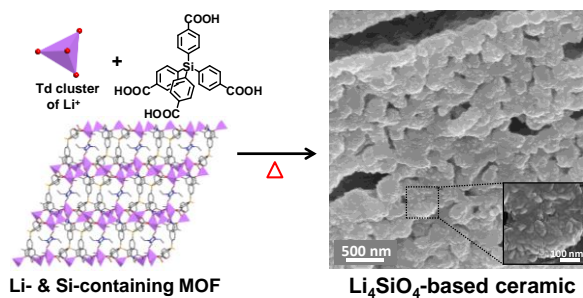
Thermal conversion of a Li- and Si-containing MOF produces ceramic Li_4SiO_4 with a coral-like morphology, which is an advanced CO_2 absorbent with high uptake and fast absorption.

Dalton Transactions

COMMUNICATION

Thermal conversion of a tailored metal-organic framework into lithium silicate with an unusual morphology for efficient CO$_2$ capture

Jae Hwa Lee,[a] Byoungnam Moon,[a] Tae Kyung Kim,[a] Sungeun Jeoung,[a] and Hoi Ri Moon*[a]

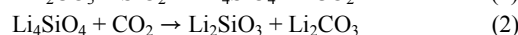**The conversion reaction of metal-organic frameworks (MOFs) was adopted as a synthetic method to produce an advanced CO$_2$ absorbent. A Li- and Si-containing MOF is a good precursor for lithium orthosilicate (Li$_4$SiO$_4$); the resulting solid has an unusual coral-like morphology, which provides an enhanced CO$_2$-sorption performance (high uptake and fast absorption).**

Anthropogenic carbon dioxide (CO$_2$) emission is considered to be one of the major reasons for global warming, which is a serious environmental threat.[1] CO$_2$ is mostly derived from the combustion of fossil fuels in power plants (approximately one-third of the emitted CO$_2$) and it is expelled as a hot gas.[2] In this regard, the capture and sequestration of CO$_2$ at high temperatures is an emerging area of research aimed at reducing the concentration of CO$_2$ in the atmosphere. Among various CO$_2$-capture materials, lithium-based ceramics such as Li$_2$ZrO$_3$, Li$_2$SiO$_3$, Li$_8$SiO$_6$, Li$_5$AlO$_4$, Li$_4$TiO$_4$, and Li$_4$SiO$_4$ have achieved recognition, because they capture CO$_2$ via chemisorption in a wide temperature range and with a high degree of recyclability.[3] Among them, lithium orthosilicate (Li$_4$SiO$_4$) is a qualified candidate for the uptake of CO$_2$ from combustion gases, because of its fast absorption kinetics and large absorption capacity (theoretical sorption amount of 36.7 wt %).[4]

Li$_4$SiO$_4$-based absorbents are conventionally synthesised by the solid-state reaction of silica with lithium salts such as LiOH and Li$_2$CO$_3$, as described in equation (1). As part of an effort to vary the types of precursors and the synthetic conditions, the impregnation-precipitation process[5] and sol-gel synthesis[6] have been used for the synthesis of Li$_4$SiO$_4$, which has led to changes to its surface properties and to an increase of its surface area. Because CO$_2$ molecules react with Li$^+$ and O^{2-} ions diffused from inside of the Li$_4$SiO$_4$ absorbent on the surface[7] according to equation (2), those efforts were effective for enhancing the CO$_2$-capture performances. Therefore, various attempts with new precursors and methods are meaningful to develop absorbents with good performances.

$$2Li_2CO_3 + SiO_2 \rightarrow Li_4SiO_4 + 2CO_2 \qquad (1)$$
$$Li_4SiO_4 + CO_2 \rightarrow Li_2SiO_3 + Li_2CO_3 \qquad (2)$$

Recently, a novel synthetic method, using a conversion reaction of metal-organic frameworks (MOFs) as precursors, has been introduced and recognised for the preparation of advanced materials.[8,9] This method imparts the materials with unprecedented nanostructures and/or porous architectures, and the resulting materials exhibit outstanding performances in numerous applications such as catalysts, gas storage, and electrodes. Since a MOF is an extended network of metal ions/clusters coordinated by multidentate organic ligands, the well-dispersed metal ions are easily converted back into metallic materials by simple chemical or thermal decomposition processes whereby ligands are removed or carbonised. The synthetic products are generally nanoporous and/or nanocrystalline due to the sacrificial template effect of the original MOF lattice; these are essential characteristics of excellent sorbents or catalysts.[10] Therefore, the conversion reaction of MOFs is a synthetic method that affords inorganic materials with novel properties. In particular, because ceramics that require solid-state reactions at high temperatures hardly allow for control of the morphologies, the implementation of a method to convert MOFs into ceramics enables ceramics to possess various interesting morphologies.
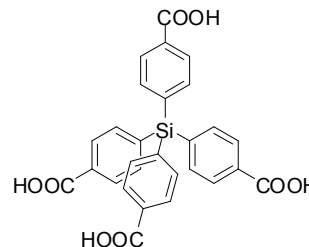

Fig. 1 Tetrakis(4-carboxyphenyl)silane (H$_4$TCS).

In this work, a newly designed MOF, containing Li and Si atoms, was synthesised and used as a precursor. This MOF was thermally converted into Li_4SiO_4, which has a coral-like morphology; its unique structural properties enhance its CO_2-sorption behaviour. We attribute these features to the MOF precursor and its thermal conversion reaction. To construct a MOF containing Li and Si atoms in a 4:1 ratio, it is important to introduce an appropriate organic building block. In this sense, tetrakis(4-carboxyphenyl)silane (H_4TCS) is a proper ligand.[11] It is a Si-centred tetracarboxylic acid ligand (Fig. 1); the electronic charge of the derived tetracarboxylate can be balanced by four Li^+ ions. The solvothermal reaction of
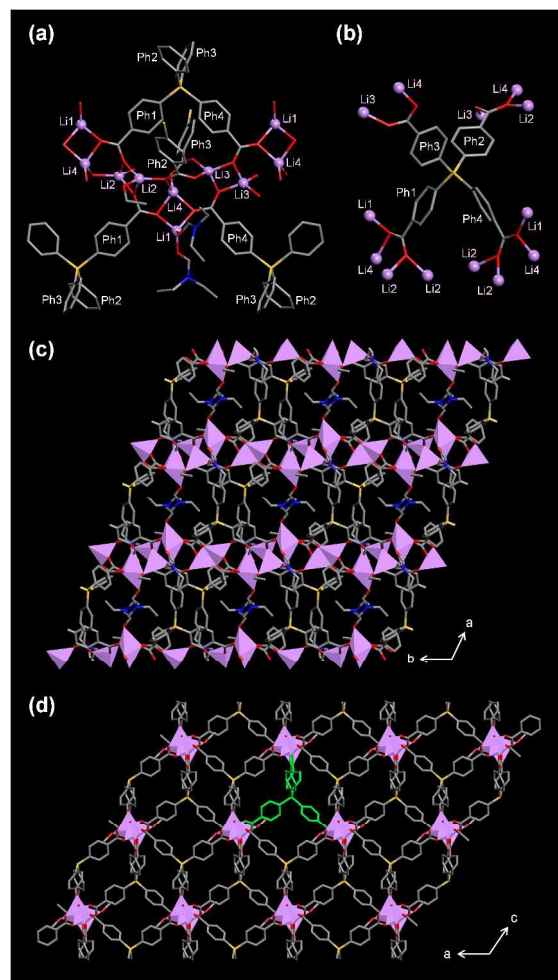

Fig. 2 Single-crystal X-ray structure of LiTCS. (a) Secondary building units (SBUs) of the Li-COO chain. (b) The coordination modes of the carboxylates of a TCS^{4-} ligand. Three-dimensional framework formed by SBUs and organic ligands, projected along (c) the c axis and (d) the b axis. Coordinating DEF molecules and Li1 in Fig 2d were omitted for clarity. (Colour scheme: C, grey; O, red; N, blue; Si, orange; Li, purple.)

$LiNO_3 \cdot 6H_2O$ with H_4TCS in a mixture of N,N-diethylformamide (DEF) and ethanol (EtOH) yielded yellowish block-shaped crystals of $[Li_4(TCS)(DEF)_2(EtOH)]\cdot 0.25EtOH \cdot H_2O$ (LiTCS). The structure of LiTCS, determined by single-crystal X-ray diffraction (Table S1), consists of one TCS ligand, four lithium ions, two coordinating DEF molecules, and one coordinating EtOH molecule per asymmetric

unit. All of the Li^+ ions have distorted tetrahedral geometries (Fig. 2a and Table S2): Li3 and Li4 are bonded to carboxylate oxygen atoms associated with four different TCS^{4-} moieties. Li1 is coordinated by two carboxylates and two DEF molecules. Li2 is coordinated by three carboxylates and one EtOH molecule. As shown in Fig. 2b, among the various possible bridging modes of carboxylate ligands, the carboxylates belonging to Ph1 and Ph4 display μ_4-η^2:η^2 modes, the carboxylate from Ph2 displays a μ_3-η^1:η^2 mode, and the carboxylate from Ph3 shows a μ_2-η^1:η^1 mode. The infinite coordination in these modes generates one-dimensional [Li-COO] chains as secondary building units along the b axis (Fig. 2c). Because the central Si atom of a TCS ligand has a tetrahedral geometry, the TCS ligand is expected to act as a tetrahedral node. However, in the present MOF, because two carboxylates (belonging to Ph1 and Ph4) in a TCS ligand coordinate to the intrachain Li ions, the two other carboxylates extend to coordinate to two neighbouring [Li-COO] chains (Fig. 2d). Thus, this ligand is a three-way junction to generate a three-dimensional (3D) network. Because of the pore blockage of two coordinating DEF molecules, this 3D MOF possesses 1D channels (Figs. 2c and 2d). The X-ray powder diffraction (XRPD) pattern of the as-synthesised LiTCS is consistent with the simulated pattern derived from the single-crystal diffraction data (Fig. S1), indicating that the bulk and single crystals are the same material.
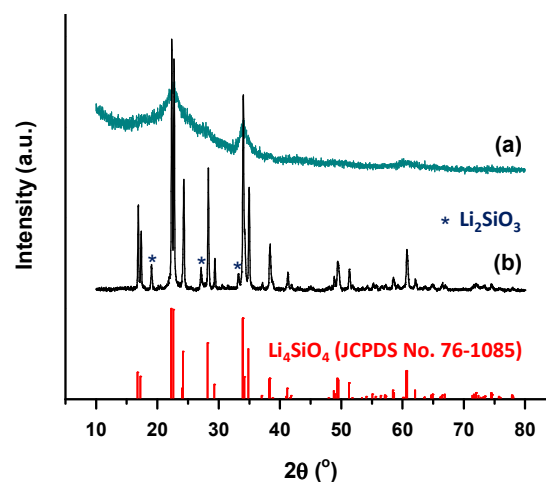

Fig. 3 XRPD patterns of the as-synthesised Li_4SiO_4 (a) before and (b) after thermolysis under air at 650 °C.

Thermogravimetric analysis (TGA) indicated that LiTCS thermally decomposes above ca. 550 °C (Fig. S2). Because the conventional synthesis of Li_4SiO_4 is conducted at 600–900 °C, the grinded yellowish crystals of LiTCS were heated at 700 °C for 6 h in a tube furnace under a nitrogen flow of 250 mL/min. As shown in Fig. 3a, XRPD data for the resulting black powder show broad peaks that coincide with those measured for Li_4SiO_4 (JCPDS No. 76-1085). The relatively low crystallinity might originate from a large amount of carbon residue (49 wt %, based on elemental analysis) due to incomplete reaction (Fig. S3). Further heat treatment under air at 650 °C for 2 h (Fig. S3) consequently resulted in highly crystalline white product, displaying the sharp XRPD pattern (Fig. 3b) of Li_4SiO_4 (trace amounts of Li_2SiO_3 were present). Despite the high

annealing temperature, a small amount of carbon (~1.3 wt %) was still detected; this may be attributed to unburned carbon in the solid and/or to lithium carbonate on the surface.
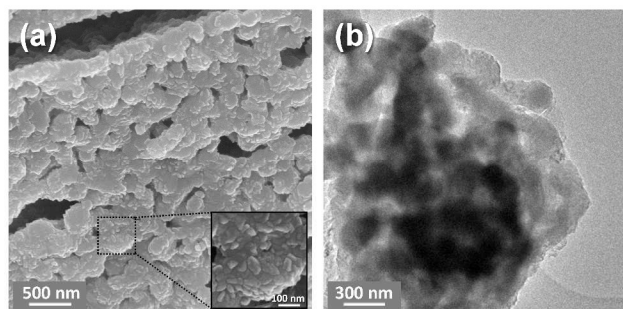

Fig. 4 (a) SEM and (b) TEM images of as-synthesised Li_4SiO_4, showing its coral-like morphology.

The morphology of the prepared Li_4SiO_4 was investigated by scanning electron microscopy (SEM) and transmission electron microscopy (TEM). The SEM images (Figs. 4a and S4-5) reveal the loss of original LiTCS morphology and the formation of large cracks in the solid, which is presumably caused by volume shrinkage in going from LiTCS to Li_4SiO_4 (1057.9 to 82.4 Å^3, based on the volume for each formula containing one Si) and by the liberation of organic components during the thermal conversion. Interestingly, the resulting solid of Li_4SiO_4 has a coral-like morphology, constructed by the connection of secondary particles with relatively uniform dimensions (ca. 300 nm). The coarse integration of the secondary particles results in voids, corresponding to macropores. Thus, even though the nitrogen adsorption/desorption experimental results indicated a low surface area (Brunauer–Emmett–Teller surface area of 8 m^2/g), the material's macroporosity helps the mass transport of gas during CO_2 capture, thus enhancing the uptake rate and amounts. High-magnification SEM and TEM images, for closer observation, show that each secondary particle is composed of primary particles of 20–50 nm (Figs. 4a (inset) and 4b). It should be noted that the present Li_4SiO_4 has a unique morphology which cannot be achieved by conventional synthetic methods (experimental details in the ESI).[4] As shown in Fig. S6, Li_4SiO_4 is usually in the form of large agglomerates, forming a rock-like bulk solid. In contrast, the coral-like morphology of the Li_4SiO_4 reported herein is attributed to the self-templating effect of the MOF. We have previously suggested that organic substances generated during the thermal decomposition of the MOF are confined to act as templates;[8] afterwards, they are converted into nanopores. Accordingly, the conversion reaction of MOFs can be a facile and successful method to impart metal oxides with interesting architectures; this is especially true for ceramics, which require high reaction temperatures.

To verify the advantages of the special morphology of Li_4SiO_4 with regard to CO_2 capture, CO_2-absorption experiments were conducted using a TGA apparatus. Fig. 5a displays the dynamic thermogram measured at a heating rate of 5 °C/min and a flow of 15% (v/v) CO_2 in N_2, which mimics flue gas. This trace displays CO_2 chemisorption around 500 °C, accompanied by a small sorption peak below 300 °C (2.6 wt %; the blue asterisk in Fig. 5a), which is due to the reaction of Li_2SiO_3 with CO_2.[12] The actual CO_2-chemisorption
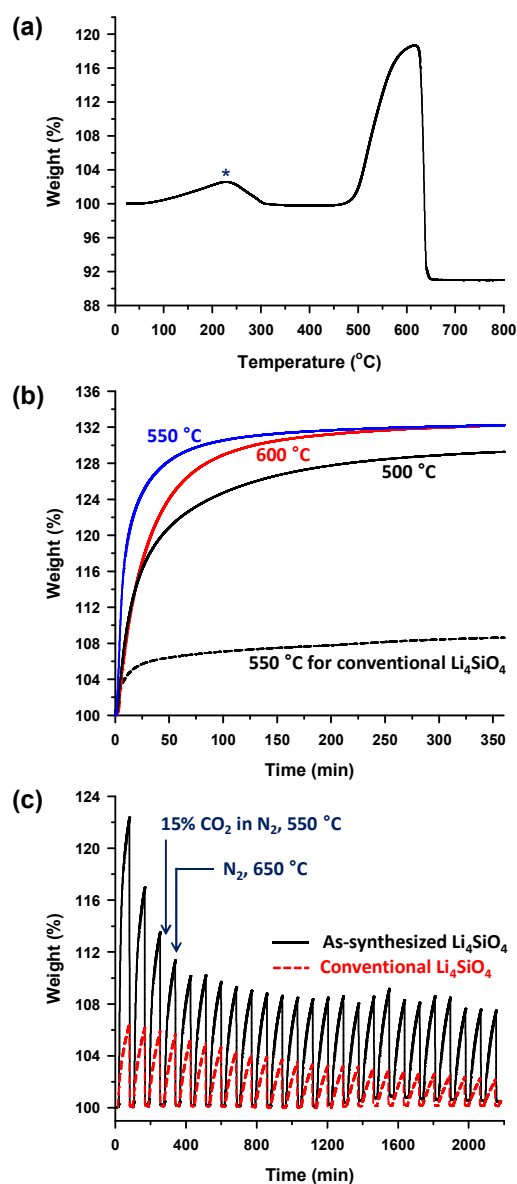

Fig. 5 (a) TG curves of Li_4SiO_4 obtained at a heating rate of 5 °C/min in 15% CO_2 balanced with N_2. (b) Change in mass uptake of Li_4SiO_4 over time at different temperatures with a flow of 15% (v/v) CO_2 in N_2. (c) Gas-cycling result of the absorbent.

process of Li_4SiO_4 begins at 455 °C and reaches the apex of 18.7 wt % at 620 °C, at which absorption and desorption are in equilibrium. At higher temperatures, the absorbed CO_2 molecules in this Li_4SiO_4 are liberated, resulting in a loss of 27.7 wt %. More mass loss relative to the initial weight (ca. 9 wt %) results from the decomposition of remaining carbon species as well as from the dissociation of CO_2 from the pre-existing Li_2CO_3 in the as-synthesised Li_4SiO_4, as mentioned previously. To examine the temperature dependence of the CO_2-absorption behaviour of Li_4SiO_4, the absorbent was monitored isothermally under flowing mimicked flue gas at 500, 550, and 600 °C for 6 h (Fig. 5b). At 500 °C, the uptake of Li_4SiO_4 shows a relatively slow saturation to 29.4 wt %. The ultimate CO_2-uptake amounts at 550 and 600 °C similarly approach 32.4 wt %, which corresponds to 88% of the theoretical capacity of Li_4SiO_4. However,

the initial absorption rates at 550 and 600 °C are significantly different: during the first 5 min, while 12.0 wt % uptake occurs at 550 °C, only 3.5 wt % uptake occurs at 600 °C. The Li_4SiO_4 reported herein shows a CO_2-sorption behaviour superior to that of Li_4SiO_4-based absorbents previously prepared by the conventional solid-state synthesis (maximum uptake at 550 °C of 7.8 wt %; 3.3 wt % uptake at 550 °C after 5 min) (dotted line in Fig. 5b). The stability of the coral-like Li_4SiO_4 was also tested by cyclic absorption/desorption experiments. Absorption was performed with 15% CO_2 in N_2 at 550 °C and desorption was performed under pure N_2 at 650 °C. The experimental results indicate a severe decay of the absorption amounts during the first four cycles, decreasing from 22.4 wt % to 11.4 wt %. After 25 cycles, the CO_2-absorption/desorption processes converged to 7.7 wt %, which is a third of the uptake of the first cycle. SEM images of the solid at the end of the experiment show that the porous coral-like morphology had mostly collapsed (Fig. S7). This result indicates that the deterioration of the CO_2-capture capacity is directly related to the destruction of the material's morphology. The same cyclic test for the morphologically featureless rock-like Li_4SiO_4, meanwhile, displayed a gradual decline of the absorption capacity from 6.5 wt % to 2.2 wt % over the 25 cycles (dotted red line in Fig. 5c). The result implies there might be other factors that have a bad influence on the reversibility of the CO_2 absorption processes in addition to t the morphological change. However, since the coral-like sample shows the much larger degradation of absorption capacity during the cycles, it can be said that the enhanced CO_2-uptake capacity is surely caused by the coral-like morphology generated during the MOF conversion, which has a significant effect on the absorption rate and capacity. As a result, the development of absorbents showing advanced and robust morphologies will be a further important direction of this research.

Conclusions

LiTCS, which is a tailored MOF containing Si and Li atoms, was synthesised and used as a precursor for Li_4SiO_4. This MOF-conversion method resulted in a coral-like morphology of Li_4SiO_4, which can hardly be achieved by the conventional synthetic approach. The as-prepared Li_4SiO_4 showed CO_2-absorption behaviour superior to that of other materials, having a much higher uptake amount and faster absorption. This might be attributed to its interesting coral-like morphology, providing a passage for the mass transport of gas and a high surface area for effective interaction. Therefore, this novel approach of MOF conversion can be a new route toward useful metal oxides (especially ceramics) with interesting architectures and advanced properties.

Acknowledgements

Notes and references

[a] Department of Chemistry, Ulsan National Institute of Science and Technology (UNIST), 50 UNIST-gil, Ulsan 689-798, Republic of Korea. E-mail: hoirimoon@unist.ac.kr.

† Electronic Supplementary Information (ESI) available: Experimental details, crystallographic data, XRPD patterns, TGA traces, SEM and TEM images. CCDC 1049388. See DOI: 10.1039/c000000x/

‡ Crystal data of LiTCS: $C_{40}H_{44}Li_4N_2O_{11}Si$, M_r = 784.62, triclinic, space group P-1 (no. 2), a = 13.725(3) Å, b = 14.074(3) Å, c = 14.187(3) Å, α = 114.15(3)°, β = 114.20(3)°, γ = 98.24(3)°, V = 2115.7(10) Å^3, Z = 2, d_{calcd} = 1.232 g cm^{-3}, T = 100(2) K, crystal size 0.11 x 0.12 x 0.17 mm^3, λ = 0.64999 Å, 2θ = 24.347, 552 parameters, R_1 = 0.0577 (I>2σ(I), 7301 reflections), wR_2 = 0.1816 (all data, 8489 reflections), GOF = 1.075.

1   K. M. K. Yu, I. Curcic, J. Gabriel and S. C. E. Tsang, *ChemSusChem*, 2008, **1**, 893.
2   (*a*) S, Choi, J. H. Drese and C. W. Jones, *ChemSusChem*, 2009, **2**, 796; (*b*) B. N. Nair, R. P. Burwood, V. J. Goh, K. Nakagawa and T. Yamaguchi, *Prog. Mater. Sci.*, 2009, **54**, 511.
3   (*a*) N. Togashi, T. Okumura and K. Oh-ishi, *J. Ceram. Soc. Jpn.*, 2007, **115**, 324; (*b*) R. Rodríguez-Mosqueda and H. Pfeiffer, *J. Phys. Chem. A*, 2010, **114**, 4535; (*c*) T. Ávalos-Rendón, J. Casa-Madrid and H. Pfeiffer, *J. Phy. Chem. A*, 2009, **113**, 6919; (*d*) Q. Xiao, Y. Liu, Y. Zhong and W. Zhu, *J. Mater. Chem.*, 2011, **21**, 3838; (*e*) B. Zhang, M. Nieuwoudt and A. J. Easteal, *J. Am. Ceram. Soc.*, 2008, **91**, 1927; (*f*) F. durán-Muñoz, I. C. Romero-Ibarra and H. Pfeiffer, *J. Mater. Chem. A*, 2013, **1**, 3919.
4   (*a*) H. Xu, W. Cheng, X. Jin, G. Wang, H. Lu, H. Wang, D. Chen, B. Fan, T. Hou and R. Zhang, *Ind. Eng. Chem. Res.*, 2013, **52**, 1886; (*b*) I. Romero-Ibarra, J. Ortiz-Landeros and H. Pfeiffer, *Thermochimica Acta*, 2013, **567**, 118.
5   (*a*) S.Y. Shan, S.M. Li, Q.M. Jia, L.H. J, Y.M. Wang and J.H. Peng, *Ind. Eng. Chem. Res.*, 2013, **52**, 6941; (*b*) V. L. Mejía-Trejo, E. Fregoso-Israel and H. Pfeiffer, *Chem. Mater.*, 2008, **20**, 7171.
6   (*a*) P. V. Subha, B. V. Nair, P. Hareesh, A. P. Mohamed, T. Yamaguchi, K. G. K. Warrier and U. S. Hareesh, *J. Mater. Chem. A*, 2014, **2**, 12792; (*b*) X. Wu, Z. Wen, X. Xu, X. Wang and J. Lin, *J. Nucl. Mater.*, 2009, **392**, 471.
7   Z. Qi, H. Daying, L. Yang, Y. Qian and Z. Zibin, *Am. Inst. Chem. Eng.*, 2013, **59**, 901.
8   (*a*) J. H. Lee, Y. J. Sa, T. K. Kim, H. R. Moon and S. H. Joo, *J. Mater. Chem. A*, 2014, **2**, 10435; (*b*) K. J. Lee, T.-H. Kim, T. K. Kim, J. H. Lee, H.-K. Song and H. R. Moon, *J. Mater. Chem. A*, 2014, **2**, 14393; (*c*) T. K. Kim, K. J. Lee, J. Y. Cheon, J. H. Lee, S. H. Joo and H. R. Moon, *J. Am. Chem. Soc.*, 2013, **135**, 8940.
9   (*a*) M. Y. Maoomi and A. Morsali, *Cood. Chem. Rev.*, 2012, **256**, 2921; (*b*) S. J. Yang, T. Kim, J. H. Im, Y. S. Kim, K. Lee, H. Jung and C. R. Park, *Chem. Mater.*, 2012, **24**, 464; (*c*) C. W. Abney, K. M. L. Taylor-Pashow, S. R. Russell, Y. Chen, R. Samantaray, J. V. Lockard and W. Lin, *Chem. Mater.*, 2014, **26**, 5231; (*d*) B. Liu, H. Shioyama, T. Akita and Q. Xu, *J. Am. Chem. Soc.*, 2008, **130**, 5390; (*e*) H.-L. Jiang, B. Liu, Y.-Q. Lan, K. Kuratani, T. Akita, H. Shioyama, F. Zong and Q. Xu, *J. Am. Chem. Soc.*, 2011, **133**, 11854.

10 (*a*) M. E. Davis, *Nature*, 2002, **417**, 813; (*b*) H. Yang and D. Zhao, *J. Mater. Chem.*, 2005, **15**, 1217; (*c*) Y. Ren, Z. Ma and P. G. Bruce, *Chem. Soc. Rev.*, 2012, **41**, 4909; (*d*) D. Gu and F. Schüth, *Chem. Soc. Rev.*, 2013, **43**, 313.

11 H. Yu, M. Tian, C. Shen and Z. Wang, *Polym. Chem.*, 2013, **4**, 961-968.

12 (*a*) J. Ortiz-Landeros, C. Gómez-Yáñez and H. Pfeiffer, *J. Solid State Chem.*, 2011, **184**, 2257; (*b*) E. Ochoa-Fernandez, T. Zhao, M. Ronning and D. Chen, *J. Environ. Eng.*, 2009, **135**, 397.

Dalton Transactions Accepted Manuscript